RSC Advances

PAPER

View Article Online
View Journal | View Issue

Cite this: *RSC Adv.*, 2022, **12**, 13448

Rapid electrochemical quantification of trace Hg^{2+} using a hairpin DNA probe and quantum dot modified screen-printed gold electrodes†

Wancun Zhang,[a] Pin Zhang,[a] Ying Liang,[a] Weyland Cheng,[a] Lifeng Li,[a] Huanmin Wang,[a] Zhidan Yu,*[a] Yan Liu*[b] and Xianwei Zhang *[b]

Rapid, simple, sensitive and specific approaches for mercury(II) (Hg^{2+}) detection are essential for toxicology assessment, environmental protection, food analysis and human health. In this study, a ratiometric hairpin DNA probe based electrochemical biosensor, which relies on hairpin DNA probes conjugated with water-soluble and carboxyl functionalized quaternary Zn–Ag–In–S quantum dot (QD) on screen-printed gold electrodes (SPGE), referred to as the HP-QDs-SPGE electrochemical biosensor in this study, was developed for Hg^{2+} detection. Based on the "turn-off" reaction of a hairpin DNA probe binding with a mismatched target and Hg^{2+} through the formation of T–Hg^{2+}–T coordination, the HP-QDs-SPGE electrochemical biosensor can rapidly quantify trace Hg^{2+} with high ultrasensitivity, specificity, repeatability and reproducibility. The conformational change of the hairpin DNA probe caused a significant decrease in electrochemical intensity, which could be used for the quantification of Hg^{2+}. The linear dynamic range and high sensitivity of the HP-QDs-SPGE electrochemical biosensor for the detection of Hg^{2+} was studied *in vitro*, with a broad linear dynamic range of 10 pM to 1 μM and detection limits of 0.11 pM. In particular, this HP-QDs-SPGE electrochemical biosensor showed excellent selectivity toward Hg^{2+} ions in the presence of other metal ions. More importantly, this biosensor has been successfully used to detect Hg^{2+} in deionized water, tap water, groundwater and urine samples with good recovery rate and small relative standard deviations. In summary, the developed HP-QDs-SPGE electrochemical biosensor exhibited promising potential for further applications in on-site analysis.

Received 21st March 2022
Accepted 18th April 2022

DOI: 10.1039/d2ra01817a

rsc.li/rsc-advances

1. Introduction

In recent decades, man-made contamination has led to the release of a large amount of pollutants such as heavy metal ions into the aquatic environment through poorly controlled industrial and urban wastewaters.[1] Highly toxic, non-biodegradable, and carcinogenic heavy metals such as mercury can seriously threaten the sustainability of aquatic resources. Water-soluble mercury ions (Hg^{2+}) are the most stable form of mercury pollution due to their high toxicity and bioaccumulation. Hg^{2+} can be converted into methylmercury and accumulate in the body, causing various disorders and irreversible damage to the endocrine system, liver, kidneys, brain, nervous system, *etc.* The contamination of drinking water and other natural water resources is a significant problem as even trace amounts of Hg^{2+} can threaten human health.[2–5] Therefore, strategies for rapid, simple, sensitive, and specific detection of Hg^{2+} are imperative in order to remain below the upper limit of 10 nM Hg^{2+} in drinking water, a standard set by the U.S. Environmental Protection Agency (U.S. EPA).[6,7]

To date, several traditional methods have been created to measure Hg^{2+} quantity, including atomic absorption/emission spectroscopy,[8,9] cold vapour atomic fluorescence spectroscopy,[10,11] X-ray fluorescence spectrometry[11,12] and inductively coupled plasma-mass spectrometry.[13] These techniques are sensitive and accurate, but usually require expensive and sophisticated instrumentation, which limits their application in routine measurements.

Ono and Togashi found that Hg^{2+} can interact specifically with thymine bases (T) in two DNA strands to form a stable T–Hg^{2+}–T structure, which is even more stable than the Watson-Crick adenine-thymine pair.[14–16] Consequently, T–T base pairs have been widely used to develop Hg^{2+} biosensors using transduction mechanisms such as fluorescence,[14,15] colorimetry,[17,18] electrochemiluminescence[19] and electrochemistry.[5,6,20] Among those approaches, electrochemical-based approaches have attracted substantial interest due to the advantages of high

[a]*Henan Key Laboratory of Children's Genetics and Metabolic Diseases, Zhengzhou Key Laboratory of Precise Diagnosis and Treatment of Children's Malignant Tumors, Children's Hospital Affiliated to Zhengzhou University, Zhengzhou 450018, China. E-mail: zhidanyu2013@126.com; Fax: +86-373-63866536; Tel: +86-373-63866536*

[b]*Department of Medicine, The First Affiliated Hospital of Zhengzhou University, Zhengzhou, China. E-mail: zhangxw956658@126.com; lyJenny106@163.com*

† Electronic supplementary information (ESI) available. See https://doi.org/10.1039/d2ra01817a

sensitivity, high specificity, simple, rapid operation, low cost and suitability for miniaturization when combined with micromachining technologies.[21–23] However, it is still necessary to prepare an ultrasensitive electrochemical sensor with a simple preparation process for the ultrasensitive quantification of trace Hg^{2+}.

The detection performance of electrodes can be further improved by incorporating advanced materials into the electrode manufacturing and electrode modification process.[21–24] In general, electrochemical performance is strongly impacted by the effectiveness of electrode materials. Noble metal nanoparticles and carbon-based materials (gold-based materials, silver-based materials, carbon nanotubes, carbon fibers) have been used for the detection of Hg^{2+}.[25–27] Among these materials, gold electrode is highly attractive for the electrochemical detection of Hg^{2+}. For example, Mandler *et al.* revealed that gold nanoparticles could serve as nucleation sites for the deposition of Hg^{2+}, thus facilitating the detection of Hg^{2+} using an electrochemical based approach.[28] Zhonggang Liu *et al.* reported on the facile fabrication of electrosynthesized FeOOH nanoflakes on nanoporous gold (NPG) microwires. An exceptional electrochemical performance was achieved with a high sensitivity of 123.5 $\mu A\ \mu M^{-1}\ cm^{-2}$ and low detection limit of 7.81 nM.[25] Gold electrodes with different morphologies were also applied as efficient substrates for the determination of Hg^{2+}.[29–31] However, gold electrodes have a high cost and need to be pretreated before use. Upon damage, gold electrodes are also difficult to regenerate. In recent years, electrochemical sensors developed based on screen printed gold electrodes (SPGE) can resolve these problems. SPGE is a disposable electrode which integrates a working electrode, reference electrode and auxiliary electrode. It has the advantages of being simple to manufacture and mass production, low cost, easy to carry, convenient to operate and requiring less sample consumption. It can effectively solve the problem of cross interference when multiple samples are detected by sharing the same electrode.[32–35]

For bio-sensing electrodes, quantum dots (QDs) are an excellent choice due to their oxygen-rich functional groups, remarkable quantum confinement, edge effects, conductivity, stability, biocompatibility, and large surface area. In particular, QDs provide abundant carboxyl groups at the surface, which can be used to link amino modified DNA probes.[27,36,37] Our previous work successfully synthesized water-soluble and carboxyl functionalized quaternary Zn–Ag–In–S QDs using a facile aqueous synthesis approach that was less toxic due to the absence of highly toxic cadmium.[38] The prepared Zn–Ag–In–S QDs exhibited excellent stability in water, which made it possible for uniform electrode surface modification.

Therefore, considering the advantages of gold-based nanomaterials and Zn–Ag–In–S QDs, we developed an efficient electrochemical biosensor based on SPGE and QDs for the detection of Hg^{2+} in environmental samples. The innovation of this work is summarized as follows: (1) hairpin DNA probes specifically bind with Hg^{2+} through the formation of T–Hg^{2+}–T coordination and can provide rapid, sensitive and specific quantification of trace Hg^{2+} with high repeatability and reproducibility. (2) The water-soluble and carboxyl functionalized quaternary Zn–Ag–In–S QDs coated on a SPGE can increase the conductivity, stability, biocompatibility, and surface area of the developed test. Given the speed, high sensitivity, simplicity, and convenience of operation, the developed test serves as a potential alternative tool for Hg^{2+} determination in toxicological assessment, environmental protection and food analysis.

2. Experimental section

2.1. Reagents, materials, and instruments

All DNA used in this study was purchased from Sangon Biotech (Shanghai, China) and all sequences are listed in Table S1.† Diethyl pyrocarbonate (DEPC) treated water was obtained from TaKaRa Biotechnology (Dalian, China). Zn–Ag–In–S QDs was synthesized and referenced in our previous report.[38] 10 × Nt.BstNBI buffer (25 mM Tris–HCl (pH 7.9), 50 mM NaCl, 5 mM $MgCl_2$, and 0.5 mM dithiothreitol), 10× ThermoPol buffer (20 mM Tris–HCl (pH 8.8), 10 mM KCl, 10 mM $(NH_4)_2SO_4$, 2 mM $MgSO_4$, 0.1% Triton X-100, and tris-2-amino-2-hydroxymethyl propane-1,3-diol) were purchased from New England Biolabs. Nitric acid, mercury nitrate, *N*-hydroxysuccinimide (NHS), 1-ethyl-3-(3-dimethylaminopropyl)carbodiimide hydrochloride (EDC), and other chemicals of analytical grade purity were obtained from Aladdin (Shanghai, China) (**http://www.aladdin-e.com**). 0.2% nitric acid was used to dissolve mercury nitrate, and then uses 0.1 M PBS (sodium dihydrogen phosphate and disodium hydrogen phosphate) to dilute different concentrations. For the production of SPGE, the designed electrode pattern was printed on a 96% alumina ceramic substrate using a 0.9999 purity gold paste by screen printing, and the counter electrode was gold and the reference electrode was Ag/AgCl material, the working electrode diameter is 3 mm.

Electrochemical measurements were taken using a CHI 660C electrochemical workstation (Chenhua Instrument Company, Shanghai, China, **http://www.chinstruments.com**), which consisted cyclic voltammetry (CV) and differential pulse voltammetry (DPV) at room temperature (RT, 25 ± 1 °C). CV and DPV were performed on a CHI 660C electrochemical workstation using QDs-SPGE with a diameter of 3.0 mm as the working electrode and counter electrode, Ag/AgCl electrode as the reference electrode, in a 5.0 mM $K_3Fe(CN)_6/K_4Fe(CN)_6$ (1 : 1) solution containing 0.10 M KCl at room temperature. During the electrochemical detection, the divalent iron in the $K_3Fe(CN)_6/K_4Fe(CN)_6$ is oxidized to trivalent iron, and an electron transfer occurs to form an oxidation current, that is, the oxidation peak-to-peak current. CV was measured at potentials between −0.6 V and 0.6 V, whereas DPV scans were conducted between −0.6 V and 0.4 V with a 0.004 V increment (E), 0.05 V amplitude, 0.5 s pulse width, and 0.5 s pulse period. All DPVs were baseline-corrected using the application within the CHI software package (version 9.02) and no changes in potential or peak current values were observed.

2.2. Functional modifications of gold electrode

First, 10 μL of the 0.3 mg mL^{-1} Zn–Ag–In–S QDs suspension (dissolved in water) was drop-coated onto the surface of the SPGE and subsequently dried at room temperature (QDs-SPGE). Following, 5 μL of EDC solution (5 mg mL^{-1}) and 5 μL of NHS solution (5 mg mL^{-1}) was dropped onto the surface of the QDs-SPGE for 2 h to activate the QDs carboxyl groups. Subsequently, the modified and activated QDs-SPGE was immersed in amino modified hairpin DNA probes (10 μM, 50 μL) for 2 h at room temperature to immobilize the probe *via* amide bonds (HP-QDs-SPGE). Before the electrochemical measurements, the electrode was rinsed with purified water to eliminate nonspecific adsorption and stored in N_2 atmosphere at 4 °C.

2.3. Hg^{2+} detection using electrochemical analysis

The HP-QDs-SPGE was incubated with Hg^{2+} (10 μL) and the mismatched target (100 nM, 10 10 μL) for 15 min in 0.5× Nt.BstNBI buffer and 1× ThermoPol buffer on the surface of HP-QDs-SPGE to facilitate hybridization and the formation of the T–Hg^{2+}–T coordination on the HP-QDs-SPGE (Hg^{2+}-HP-QDs-SPGE) at 37 °C. After rinsing the electrode three times, the CV and DPV scans were conducted. Consequently, the value of the peak current was employed to monitor and determine Hg^{2+} concentration at room temperature.

3. Results and discussion

3.1. Mechanism and design of the HP-QD s-SPGE electrochemical biosensor

An overview of the HP-QDs-SPGE electrochemical biosensor for Hg^{2+} detection is illustrated in Scheme 1. The electrochemical signal was achieved by Hg^{2+} induced conformational change of the designed hairpin DNA probe on the QDs-SPGE. Prior to the experiment, the secondary structure of hairpin DNA probe were predicted by Oligo Analyzer (**https://sg.idtdna.com/calc/analyzer**), where it showed a stem-loop structure (Fig. S1†). Researchers have shown that the selective binding of Hg^{2+} to T–T base pairs in DNA duplexes. As the binding of Hg^{2+} by T–T pairs is strong and highly selective, duplexes that contain a T–T pair are thermally stabilized in the presence of Hg^{2+} ions. In contrast, other heavy-metal ions, such as Cu^{2+}, Ni^{2+}, Pd^{2+} and Co^{2+}, do not show any notable effects on duplex stability. Thus, a highly selective sensor for Hg^{2+} that relies on the selective binding of Hg^{2+} with a T–T pair.[14–20] Therefore, in the presence of Hg^{2+}, the conformational hairpin DNA probe can change to linear structure, resulting the long and double-strand on the surface of QDs-SPGE. While, in the absence of Hg^{2+}, the mismatched target DNA (with five mismatched bases T) cannot open the hairpin DNA probe, resulting the short stem-loop structure on the surface of QDs-SPGE. In addition, the mass and electron transfers and diffusion of the $Fe(CN)_6^{3-}/Fe(CN)_6^{4-}$ ions onto the surface of the QDs-SPGE, which are crucial in detecting electrochemical signals, can be blocked by the electrostatic repulsion between the $Fe(CN)_6^{3-}/Fe(CN)_6^{4-}$ ions and the negatively-charged backbone phosphate groups of the DNA binding to the surface of the QDs-SPGE. In the presence of the Hg^{2+}, hybridization of the hairpin DNA probe with the mismatched target induces the DNA to form a long, double-strand, which in turn generates a weak electrochemical signal. However, in the absence of Hg^{2+}, the hairpin DNA probe cannot hybridize with the mismatched target, resulting a relatively stronger electrochemical signal. Otherwise, the amount that the electrochemical signal decreased mainly depended on the Hg^{2+} concentration in the sample. Therefore, the concentration of Hg^{2+} could be determined by monitoring electrochemical signal decrement. In summary, our HP-QDs-SPGE electrochemical biosensor utilized the hairpin DNA probe based method to detect target Hg^{2+} in a highly specific manner.

3.2. Feasibility of the HP-QDs-SPGE electrochemical biosensor

CV and DPV are efficient methods for investigating the features of modified electrode surfaces. To verify that hairpin DNA probe bound to QDs-SPGE and hybridized with Hg^{2+}, the CV responses of the bare SPGE, QDs-SPGE, HP-QDs-SPGE and Hg^{2+}-QDs-SPGE were analyzed. As shown in Fig. 1A, the bare SPGE had one of the highest peaks due to the large specific surface area and excellent electron transfer ability of SPGE (Fig. 1A black line). However, the peak current of the QDs-SPGE was lower than that of the SPGE (Fig. 1B, red line), suggesting that the QDs successfully immobilized on the surface of the SPGE. In addition, a decrease in the peak current was observed for HP-QDs-

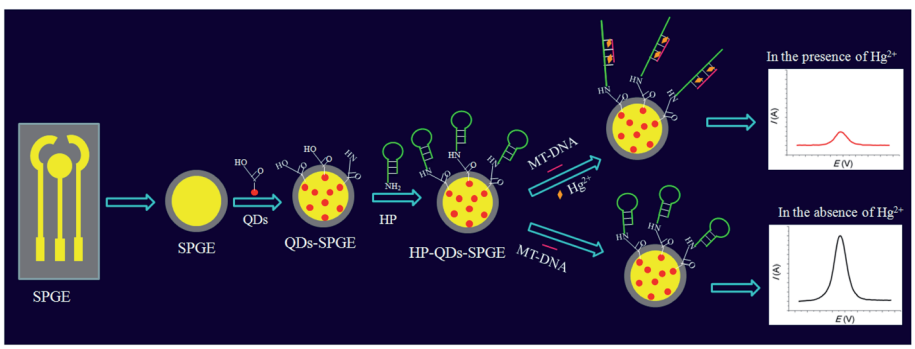

Scheme 1 Schematic illustration of the proposed HP-QDs-SPGE electrochemical biosensor.

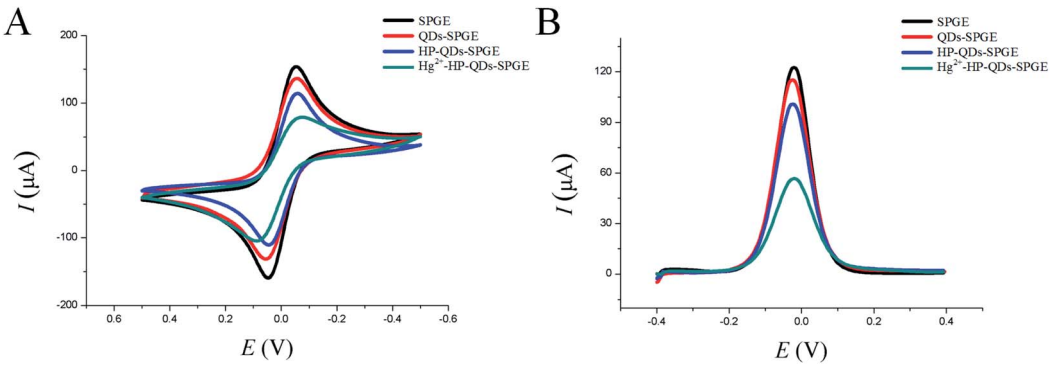

Fig. 1 The feasibility of the developed HP-QDs-SPGE electrochemical biosensor. (A) CV curves of SPGE, QDs-SPGE, HP-QDs-SPGE, and Hg^{2+}-HP-QDs-SPGE. (B) DPV curves of SPGE, QDs-SPGE, HP-QDs-SPGE, and Hg^{2+}-HP-QDs-SPGE.

SPGE (Fig. 1A blue line). This decrease can be explained by the negative charges of the hairpin DNA probe phosphate backbone, which hindered the electron transfer and mass transfer of $Fe(CN)_6^{3-/4-}$ anions on the SPGE. After hybridization among HP-QDs-SPGE, Hg^{2+} and the mismatched target DNA, a further decrease was observed in the peak current of the Hg^{2+}-HP-QDs-SPGE (Fig. 1A, green line), likely due to the repulsive electrostatic force between the negatively charged $Fe(CN)_6^{3-}/Fe(CN)_6^{4-}$ ions in the solution and the negatively charged phosphate backbone of the DNA on the surface of the SPGE. Steric hindrance in the DNA structure also reduces the electron transfer rate. Therefore, the CV signal would decrease with increasing DNA length on the electrodes. Thus, the changes in CV peak current indicated that the stepwise modification of the SPGE was successful. Furthermore, DPV was used to monitor the electrode modifications. The DPV responses of $Fe(CN)_6^{3-}/Fe(CN)_6^{4-}$ for each electrode are shown in Fig. 1B, which concur with the CV results. Therefore, the experimental results corresponded to the expected changes due to the immobilization of the hairpin DNA probe and hybridization with the mismatched target DNA. This indirectly confirms the successful modification of QDs with the hairpin DNA probe and its hybridization with the mismatched target DNA in the presence of Hg^{2+}.

3.3. Optimization of experimental parameters

To achieve optimal analytical performance, different experimental conditions of the HP-QDs-SPGE electrochemical biosensor were systematically evaluated. The hybridization temperature and hybridization time significantly affected the performance of the HP-QDs-SPGE electrochemical biosensor and were crucial for minimizing non-specific hybridization and increasing sensitivity, specificity and reproducibility. First, the hybridization temperature was optimized from 25 °C to 50 °C in the presence and absence of Hg^{2+} using the developed HP-QDs-SPGE electrochemical biosensor. As shown in Fig. 2A, in the presence of Hg^{2+}, the peak current values of the biosensor progressively decreased with increasing hybridization temperature from 25 °C to 37 °C and reached a stable electrochemical signal at 37 °C, demonstrating that the hairpin DNA probes modified on the surface of the QDs-SPGE were almost completely opened at 37 °C (Fig. 2A red line). In addition, in the absence of Hg^{2+}, the peak current values of the biosensor were almost unaltered with increasing hybridization temperature from 25 °C to 37 °C. On the other hand, with increasing hybridization temperature from 37 °C to 50 °C, the peak current values of the biosensor slightly decreased, demonstrating that the hairpin DNA probes modified on the surface of the SPGE

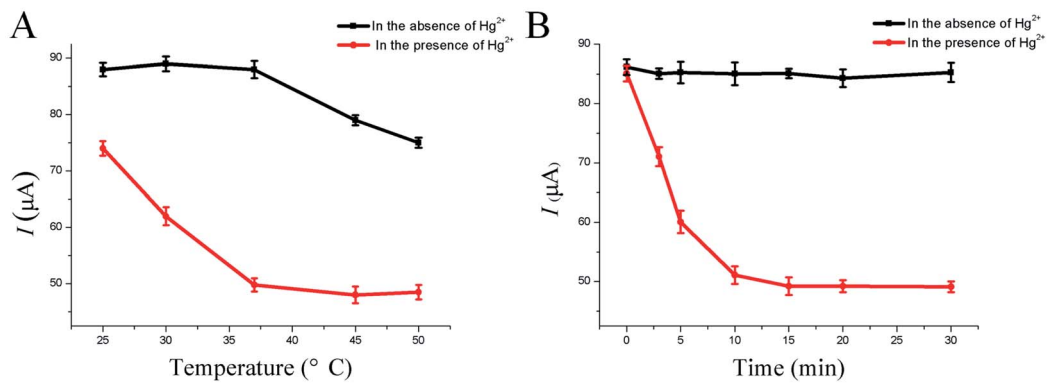

Fig. 2 The optimization results of hybrid temperature (A) and hybrid time (B) of the developed HP-QDs-SPGE electrochemical biosensor.

were opened with the increasing hybridization temperature (Fig. 2A black line). Therefore, the optimum hybridization temperature was 37 °C with an optimum hybridization time of 15 min (Fig. 2B).

3.4. Sensitivity, repeatability, and reproducibility of the HP-QDs-SPGE electrochemical biosensor

Sensitivity is an important factor to evaluate this developed HP-QDs-SPGE electrochemical biosensor due to the lower content of Hg^{2+} in real samples.[39–42] To evaluate whether the HP-QDs-SPGE electrochemical biosensor can be used to detect target sequences effectively and quantitatively, experiments were conducted with the results depicted in Fig. 3. Good linearity was obtained in 6 orders of magnitude from 0.01 nM to 1 μM Hg^{2+} using the developed HP-QDs-SPGE electrochemical biosensor. The correlation equation was $I = -7.773 \lg C - 6.7508$, (where I is the peak current and C is the concentration of Hg^{2+} in the HP-QDs-SPGE electrochemical biosensor) with a correlation coefficient $R^2 = 0.9937$ (Fig. 3A and B). Furthermore, based on the standard deviation (S_B) of seven peak current responses of the blank, the theoretical detection limit was found to be 0.11 pM, which was calculated based on the "$3S_B$/slope" ratio, where the slope of the calibration graph was taken into account. Table S2† summarizes the LOD, linear ranges, detection time, reaction step and complexity of recently reported Hg^{2+} approaches. Comparatively, the developed HP-QDs-SPGE electrochemical biosensor showed characteristics of high sensitivity, wide linear range and rapid of operation.

The repeatability of the HP-QDs-SPGE electrochemical biosensor was investigated by one individual conducting five repetitions of I measurements for 100 nM Hg^{2+} (Fig. 4A and B). The relative standard deviation (RSD) was calculated to be 1.95%, demonstrating that the repeatability of the HP-QDs-SPGE electrochemical biosensor was acceptable. Additionally, five different individuals investigated its reproducibility by performing five successive assays in the presence of 100 nM Hg^{2+}, generating an RSD of 2.66% (Fig. 4C and D). These results suggested that the HP-QDs-SPGE electrochemical biosensor could be used to quantify low levels of Hg^{2+} in real sample analysis with excellent repeatability and reproducibility.

3.5. Specificity of the HP-QDs-SPGE electrochemical biosensor

Real samples do not merely contain Hg^{2+} and often include other metal ions. Therefore, the selectivity of this HP-QDs-SPGE electrochemical biosensor for Hg^{2+} was also investigated. The selectivity of the proposed HP-QDs-SPGE electrochemical biosensor for Hg^{2+} was evaluated by exposing the sensor to an aqueous solution containing other environmentally relevant metal ions (100 nM each), such as Ca^{2+}, Co^{2+}, Cu^{2+}, Fe^{2+}, Mg^{2+}, Ni^{2+}, Zn^{2+}, Cd^{2+}, Pb^{2+} and Hg^{2+}. As shown in Fig. 5, it can be observed that in the presence of Hg^{2+} the electrochemical signal was at its lowest whereas in the presence of other metal ions, the fluorescence intensity was almost unchanged compared to the blank solution without metal ions. These results show that these competing metal ions had only negligible effects on the HP-QDs-SPGE electrochemical biosensor. The HP-QDs-SPGE electrochemical biosensor thus exhibits high selectivity for Hg^{2+}, which shows its potential for future application.

3.6. Detection of Hg^{2+} in real sample using HP-QDs-SPGE electrochemical biosensor

In order to demonstrate the practical application of the proposed HP-QDs-SPGE electrochemical biosensor in real samples, 150 nM of Hg^{2+} was added to deionized water, tap water, groundwater and urine. Trace Hg^{2+} was then detected and quantified by the HP-QDs-SPGE electrochemical biosensor. The resulting concentrations were in agreement with the spiked value with a recovery above 95.55% to 101.55% (Table 1). In summary, these results demonstrated that the proposed HP-QDs-SPGE electrochemical biosensor could accurately quantify Hg^{2+} in real samples with strong reliability, thus possessing significant potential for further application in environmental pollution detection.

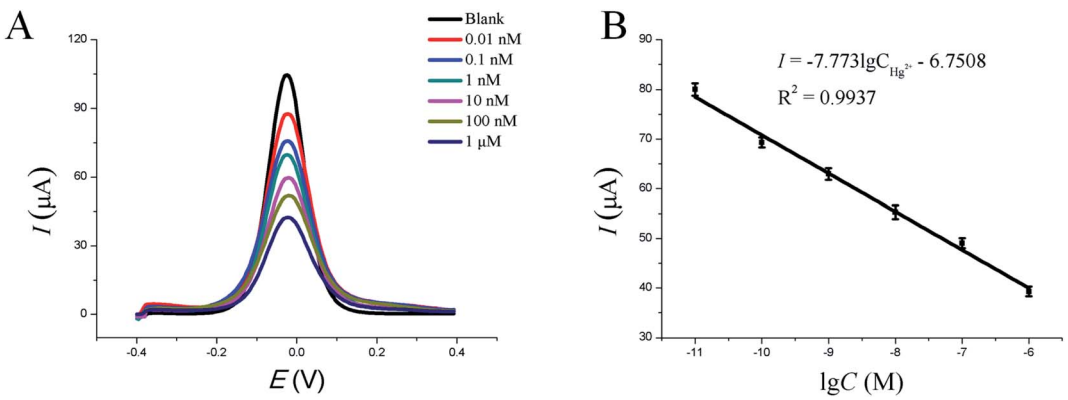

Fig. 3 The sensitivity of the developed HP-QDs-SPGE electrochemical biosensor. (A) DPVs for detection of different concentrations of Hg^{2+} using the developed HP-QDs-SPGE electrochemical biosensor. (B) The peak currents of the developed HP-QDs-SPGE electrochemical biosensor are log-linear correlations with Hg^{2+} levels in the range of 0.01 nM to 1 μM. Error bars show the standard deviation of three experiments.

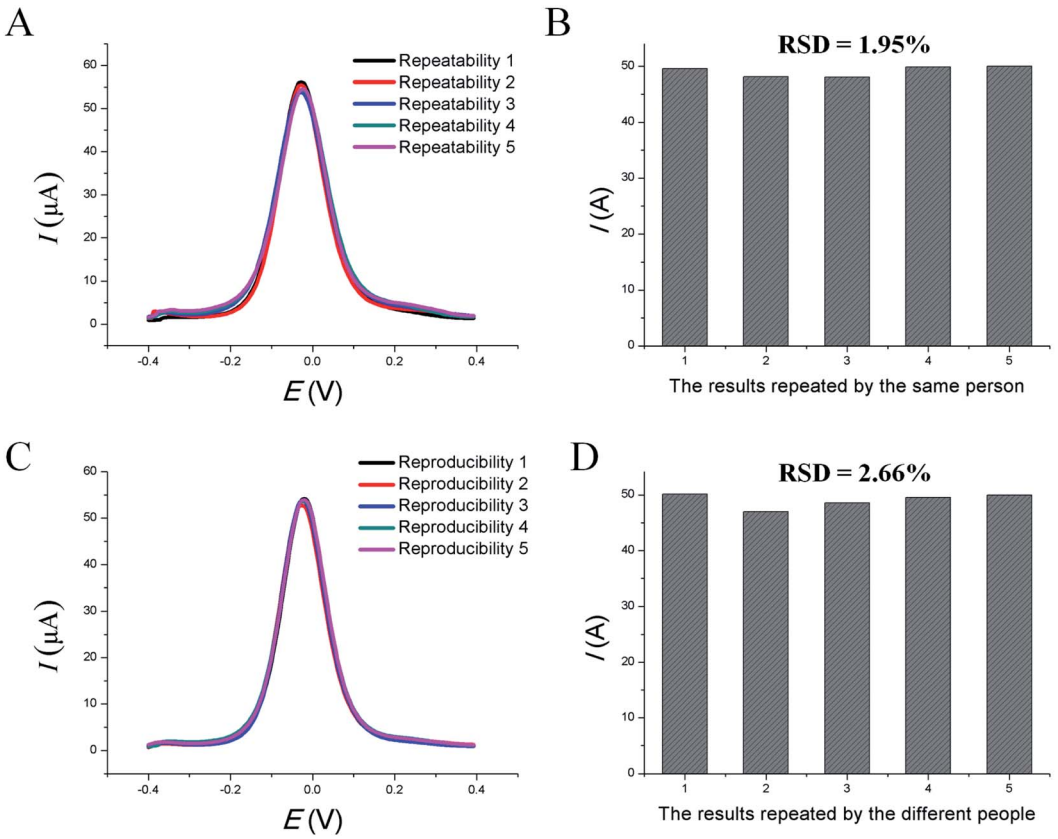

Fig. 4 (A) DPV curves and (B) corresponding histogram of repeatability results of developed HP-QDs-SPGE electrochemical biosensor. (C) DPV curves and (D) corresponding histogram of reproducibility results of developed HP-QDs-SPGE electrochemical biosensor.

Table 1 The accuracy of the developed electrochemical biosensor in real sample analysis ($n = 3$)

Name of the sample	Added (nM)	Determination value	Rate of recovery (%, $n = 3$)	Relative standard deviation (5)
Deionized water	150	152.33	101.55	2.01
Tap water	150	143.33	95.55	2.13
Groundwater	150	147.67	98.45	1.70
Urine	150	145.33	96.89	2.10

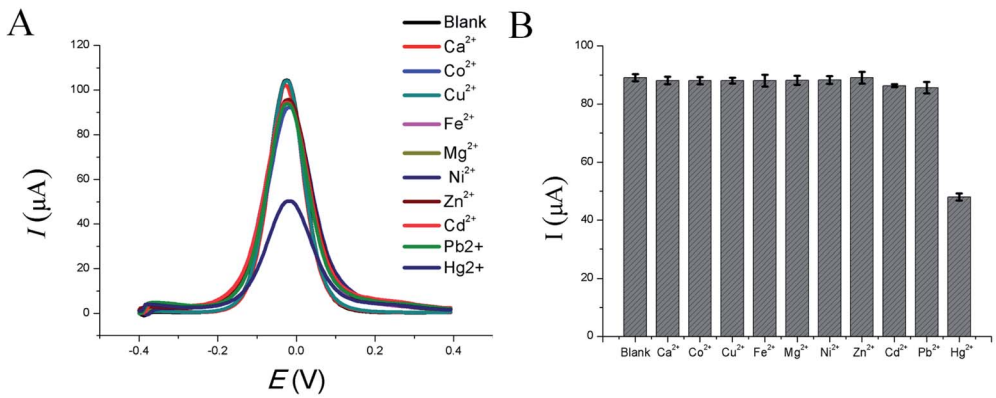

Fig. 5 The specificity results of the developed HP-QDs-SPGE electrochemical biosensor. (A) DPV curves and (B) corresponding histogram of HP-QDs-SPGE electrochemical biosensor for detection of different kinds of metal ions.

4. Conclusion

In summary, a HP-QDs-SPGE electrochemical biosensor based on a hairpin DNA probe conjugating with water-soluble Zn–Ag–In–S QDs on a SPGE, was developed for rapid and simple detection of Hg^{2+} with high sensitivity and specificity. The HP-QDs-SPGE electrochemical biosensor takes advantage of the highly selective T–Hg^{2+}–T based on conformation-switching of hairpin DNA probe with a detection limit of 0.11 pM, which is below the maximum level of mercury permitted by the US EPA for drinking water (10 nM). At the same time, the developed HP-QDs-SPGE electrochemical biosensor displayed specificity towards Hg^{2+}, even in the presence of other competitive heavy metal ions at high concentrations. More importantly, the developed HP-QDs-SPGE electrochemical biosensor could accurately quantify Hg^{2+} in real samples at a high level of reliability, which demonstrated its potential towards on-site applications of Hg^{2+} detection, during its easy to use and does not require rigorous laboratory conditions.

Author contributions

Wancun Zhang: writing – original draft, funding acquisition. Pin Zhang: formal analysis. Ying Liang: methodology. Weyland Cheng: conceptualization. Lifeng Li: resources, software. Huanmin Wang: investigation. Zhidan Yu: data curation, visualization. Yan Liu: supervision, validation. Xianwei Zhang: project administration, writing – review & editing.

Conflicts of interest

The authors declare of no conflicts of interest.

Acknowledgements

This work was supported by the China Postdoctoral Science Foundation (No. 2020M672301), scientific and technological projects of Henan province (202102310068, 222102310270), Henan medical science and technology program (LHGJ20190937 and LHGJ20190887), Henan provincial key laboratory of children's genetics and metabolic diseases foundation (SS201902 and SS201906), Henan neural development engineering research center for children foundation (SG201904 and SG201906).

References

1 I. Y. Lopez-Pacheco, A. Silva-Nunez, C. Salinas-Salazar, A. Arevalo-Gallegos, L. A. Lizarazo-Holguin, D. Barcelo, *et al.*, Anthropogenic contaminants of high concern: Existence in water resources and their adverse effects, *Sci. Total Environ.*, 2019, **690**, 1068–1088.

2 N. Safari, K. Ghanemi and F. Buazar, Selenium functionalized magnetic nanocomposite as an effective mercury(II) ion scavenger from environmental water and industrial wastewater samples, *J. Environ. Manage.*, 2020, **276**, 111263.

3 L. Yao, S. Gao, S. Liu, Y. Bi, R. Wang and H. Qu, Single-Atom Enzyme-Functionalized Solution-Gated Graphene Transistor for Real-Time Detection of Mercury Ion, *Sens. Actuators, B*, 2020, **12**, 6268–6275.

4 A. Hasan, N. Nanakali, A. Salihi, B. Rasti, M. Sharifi and F. Attar, Nanozyme-based sensing platforms for detection of toxic mercury ions: An alternative approach to conventional methods, *Talanta*, 2020, **215**, 120939.

5 G. Zeng, C. Zhang, D. Huang, C. Lai, L. Tang and Y. Zhou, Practical and regenerable electrochemical aptasensor based on nanoporous gold and thymine-Hg^{2+}-thymine base pairs for $Hg(^{2+})$ detection, *Biosens. Bioelectron.*, 2017, **90**, 542–548.

6 C. Lai, S. Liu, C. Zhang, G. Zeng, D. Huang and L. Qin, Electrochemical Aptasensor Based on Sulfur-Nitrogen Codoped Ordered Mesoporous Carbon and Thymine-Hg^{2+}-Thymine Mismatch Structure for $Hg(^{2+})$ Detection, *ACS Sens.*, 2018, **3**, 2566–2573.

7 S. Xie, Y. Tang, D. Tang and Y. Cai, Highly sensitive impedimetric biosensor for Hg^{2+} detection based on manganese porphyrin-decorated DNA network for precipitation polymerization, *Anal. Chim. Acta*, 2018, **1023**, 22–28.

8 C. Tseng, F. Martin, D. Amouroux, O. Donard and A. Dediego, Rapid determination of inorganic mercury and methylmercury in biological reference materials by hydride generation, cryofocusing, atomic absorption spectrometry after open focused microwave-assisted alkaline digestion, *J. Anal. At. Spectrom.*, 1997, **12**, 743–750.

9 D. I. Bannon, C. Murashchik, C. R. Zapf, M. R. Farfel and J. J. Chisolm, Graphite furnace atomic absorption spectroscopic measurement of blood lead in matrix-matched standards, *Clin. Chem.*, 1994, **40**, 1730–1734.

10 Y. Yu, Z. Du and J. Wang, The development of a miniature atomic fluorescence spectrometric system in a lab-on-valve for mercury determination, *J. Anal. At. Spectrom.*, 2008, **22**, 650–656.

11 A. B. Blank and L. P. Eksperiandova, Specimen preparation in x-ray fluorescence analysis of materials and natural objects, *X-Ray Spectrom.*, 1998, **27**, 147–160.

12 A. Ellis, P. Kregsamer, P. Potts, C. Streli, M. West and P. Wobrauschek, Atomic spectrometry update - X-ray fluorescence spectrometry, *J. Anal. At. Spectrom.*, 1998, **13**, 209R–232R.

13 R. J. Bowins and R. H. McNutt, Electrothermal isotope dilution inductively coupled plasma mass spectrometry method for the determination of sub-ng ml^{-1} levels of lead in human plasma, *J. Anal. At. Spectrom.*, 1994, **9**, 1233–1236.

14 H. Xu, X. Zhu, H. Ye, L. Yu, X. Liu and G. Chen, A simple "molecular beacon"-based fluorescent sensing strategy for sensitive and selective detection of mercury(II), *Chem. Commun.*, 2011, **47**, 12158–12160.

15 H. B. Teh, H. Wu, X. Zuo and S. F. Y. Li, Detection of Hg^{2+} using molecular beacon-based fluorescent sensor with high sensitivity and tunable dynamic range, *Sens. Actuators, B*, 2014, **195**, 623–629.

16 A. Ono and H. Togashi, Highly selective oligonucleotide-based sensor for mercury(II) in aqueous solutions, *Angew. Chem., Int. Ed.*, 2004, **43**, 4300–4302.

17 W. Li, Y. Li, H. L. Qian, X. Zhao, C. X. Yang and X. P. Yan, Fabrication of a covalent organic framework and its gold nanoparticle hybrids as stable mimetic peroxidase for sensitive and selective colorimetric detection of mercury in water samples, *Talanta*, 2019, **204**, 224–228.

18 J. S. Lee, M. S. Han and C. A. Mirkin, Colorimetric detection of mercuric ion (Hg^{2+}) in aqueous media using DNA-functionalized gold nanoparticles, *Angew. Chem., Int. Ed.*, 2007, **46**, 4093–4096.

19 T. L. Yuan, Z. Hu and Lianzhe, Label-free supersandwich electrochemiluminescence assay for detection of sub-nanomolar Hg^{2+}, *Chem. Commun.*, 2011, **47**, 11951–11953.

20 S. H. Wu, B. Zhang, F. F. Wang, Z. Z. Mi and J. J. Sun, Heating enhanced sensitive and selective electrochemical detection of Hg^{2+} based on T-Hg^{2+}-T structure and exonuclease III-assisted target recycling amplification strategy at heated gold disk electrode, *Biosens. Bioelectron.*, 2018, **104**, 145–151.

21 W. Zhang, F. Hu, X. Zhang, W. Meng, Y. Zhang, Y. Song, H. Wang, P. Wang and Y. Q. Gu, Ligase chain reaction-based electrochemical biosensor for the ultrasensitive and specific detection of single nucleotide polymorphisms, *New J. Chem.*, 2019, **43**, 14327–14335.

22 F. Hu, W. Zhang, W. Meng, Y. Ma, X. Zhang, Y. Xu, P. Wang and Y. Q. Gu, Ferrocene-labeled and purification-free electrochemical biosensor based on ligase chain reaction for ultrasensitive single nucleotide polymorphism detection, *Anal. Chim. Acta*, 2020, **1109**, 9–18.

23 F. Hu, W. Zhang, J. Zhang, Q. Zhang, T. Sheng and Y. Gu, An electrochemical biosensor for sensitive detection of microRNAs based on target-recycled non-enzymatic amplification, *Sens. Actuators, B*, 2018, **271**, 15–23.

24 L. Fu, A. Wang, K. Xie, J. Zhu, F. Chen and H. Wang, Electrochemical detection of silver ions by using sulfur quantum dots modified gold electrode, *Sens. Actuators, B*, 2020, **304**, 127390.

25 Z. Liu, E. Puumala and A. Chen, Sensitive electrochemical detection of Hg(II) *via* a FeOOH modified nanoporous gold microelectrode, *Sens. Actuators, B*, 2019, **287**, 517–525.

26 R. Ziółkowski, A. Uścińska, M. Mazurkiewicz-Pawlicka, A. Małolepszy and E. Malinowska, Directly-thiolated graphene based electrochemical sensor for Hg(II) ion, *Electrochim. Acta*, 2019, **305**, 329–337.

27 S. K. Arumugasamy, S. Govindaraju and K. Yun, Electrochemical sensor for detecting dopamine using graphene quantum dots incorporated with multiwall carbon nanotubes, *Appl. Surf. Sci.*, 2020, **508**, 145294.

28 N. Ratner and D. Mandler, Electrochemical detection of low concentrations of mercury in water using gold nanoparticles, *Anal. Chem.*, 2015, **87**, 5148–5155.

29 M. Zaib, M. M. Athar, A. Saeed and U. Farooq, Electrochemical determination of inorganic mercury and arsenic – a review, *Biosens. Bioelectron.*, 2015, **74**, 895–908.

30 M. Kang and B. Lee, Sensing of bisphenol A and mercury ions in aqueous solutions using a functionalized porous gold electrode, *Curr. Appl. Phys.*, 2016, **16**, 446–452.

31 T. F. Tormin, G. K. F. Oliveira, E. M. Richter and R. A. A. Munoz, Voltammetric Determination of Pb, Cu and Hg in Biodiesel Using Gold Screen-printed Electrode: Comparison of Batch-injection Analysis with Conventional Electrochemical Systems, *Electroanalysis*, 2016, **28**, 940–946.

32 R. Zribi, R. Maalej, E. Messina, R. Gillibert, M. G. Donato and O. M. Maragò, Exfoliated 2D-MoS2 nanosheets on carbon and gold screen printed electrodes for enzyme-free electrochemical sensing of tyrosine, *Sens. Actuators, B*, 2020, **303**, 127229.

33 S. Motia, B. Bouchikhi, E. Llobet and N. El Bari, Synthesis and characterization of a highly sensitive and selective electrochemical sensor based on molecularly imprinted polymer with gold nanoparticles modified screen-printed electrode for glycerol determination in wastewater, *Talanta*, 2020, **216**, 120953.

34 H. Brisset, J. F. Briand, R. Barry-Martinet, T. H. Duong, P. Frere and F. Gohier, 96X Screen-Printed Gold Electrode Platform to Evaluate Electroactive Polymers as Marine Antifouling Coatings, *Anal. Chem.*, 2018, **90**, 4978–4981.

35 A. Ganguly, J. Benson and P. Papakonstantinou, Sensitive Chronocoulometric Detection of miRNA at Screen-Printed Electrodes Modified by Gold-Decorated MoS_2 Nanosheets, *ACS Appl. Bio Mater.*, 2018, **1**, 1184–1194.

36 H. Ehzari, M. Amiri and M. Safari, Enzyme-free sandwich-type electrochemical immunosensor for highly sensitive prostate specific antigen based on conjugation of quantum dots and antibody on surface of modified glassy carbon electrode with core-shell magnetic metal-organic frameworks, *Talanta*, 2020, **210**, 120641.

37 M. Cadkova, A. Kovarova, V. Dvorakova, R. Metelka, Z. Bilkova and L. Korecka, Electrochemical quantum dots-based magneto-immunoassay for detection of HE4 protein on metal film-modified screen-printed carbon electrodes, *Talanta*, 2018, **182**, 111–115.

38 D. Deng, J. Cao, L. Qu, S. Achilefu and Y. Gu, Highly luminescent water-soluble quaternary Zn–Ag–In–S quantum dots for tumor cell-targeted imaging, *Phys. Chem. Chem. Phys.*, 2013, **15**, 5078.

39 W. Zhang, K. Liu, P. Zhang, W. Cheng, Y. Zhang, L. Li M. Chen, L. Li and X. Zhang, *All-in-one approaches for rapid and highly specific quantification of single nucleotide polymorphisms based on ligase detection reaction using molecular beacons as turn-on probes*, Talanta, 2020, p. 121717.

40 W. Zhang, F. Hu, Q. Zhang, J. Zhang, Y. Mao, P. Wang and Y. Gu, Sensitive and specific detection of microRNAs based on two-stage amplification reaction using molecular beacons as turn-on probes, *Talanta*, 2018, **179**, 685–692.

41 C. Kan, X. Shao, F. Song, J. Xu, J. Zhu and L. Du, Bioimaging of a fluorescence rhodamine-based probe for reversible detection of Hg(II) and its application in real water environment, *Microchem. J.*, 2019, **150**, 104142.

42 H. Lou, Y. Zhang, Q. Xiang, J. Xu, H. Li and P. Xu, The real-time detection of trace-level Hg^{2+} in water by QCM loaded with thiol-functionalized SBA-15, *Sens. Actuators, B*, 2012, **166–167**, 246–252.